HOKKAIDO UNIVERSITY

Title	Strong export of Antarctic Bottom Water east of the Kerguelen plateau
Author(s)	Fukamachi, Y.; Rintoul, S. R.; Church, J. A. et al.
Citation	Nature Geoscience, 3(5), 327-331 https://doi.org/10.1038/NGE0842
Issue Date	2010-05
Doc URL	https://hdl.handle.net/2115/44116
Type	journal article
File Information	NG3-5_327-331.pdf

Hokkaido University Collection of Scholarly and Academic Papers : HUSCAP

Strong export of Antarctic Bottom Water east of the Kerguelen Plateau

Y. FUKAMACHI[1*], S. R. RINTOUL[2,3,4], J. A. CHURCH[2,3,4], S. AOKI[1],
S. SOKOLOV[2,3,4], M. A. ROSENBERG[4], AND M. WAKATSUCHI[1]
[1]Institute of Low Temperature Science, Hokkaido University, Sapporo 060-0819, Japan
[2]Centre for Australian Weather and Climate Research–a partnership of the Bureau of Meteorology and CSIRO, Hobart, Tasmania 7000, Australia
[3]Wealth from Oceans Flagship, Hobart, Tasmania 7000, Australia
[4]Antarctic Climate and Ecosystem Cooperative Research Centre, Hobart, Tasmania 7001, Australia
*e-mail: yasuf@lowtem.hokudai.ac.jp

The primary paths for the export of Antarctic Bottom Water to the global ocean are the deep western boundary currents east of the Antarctic Peninsula and the Kerguelen Plateau[1]. Previous ship-based studies found evidence of the Kerguelen deep western boundary current in the distribution of water properties and velocity[2-7], but no long-term measurements exist to define the mean flow. Here we use results from a coherent array of eight current-meter moorings to reveal a narrow and intense equatorward flow extending throughout the water column. Two-year mean velocities exceed 20 cm s^{-1} at depths ~3500 m, the strongest mean deep western boundary current flow yet observed at similar depths. The mean equatorward transport of water colder than 0°C is 12.3±1.2 x 10^6 m^3 s^{-1}, partially compensated by poleward flow of 6.0 x 10^6 m^3 s^{-1} mostly across the eastern end of the array. Below 0.2°C, the net transport is 8.0 x 10^6 m^3 s^{-1}, in comparison to 1.9 x 10^6 m^3 s^{-1} in the boundary current carrying dense water from the Weddell Sea into the Atlantic north of the Falkland Plateau[8]. The results confirm that the Kerguelen deep western boundary current is a significant pathway of the deep overturning circulation.

The global overturning circulation (OC) is the dominant mechanism responsible for oceanic heat transport as a result of the large temperature difference between the upper and lower limbs of the overturning cell. The OC thus has a strong influence on climate. The deep branch of the OC is supplied by cold, dense water formed in the high latitude North Atlantic and Southern Ocean and exported from the formation regions in a global network of deep western boundary currents (DWBCs), partially compensated by recirculation gyres and slower flows in the interior of the ocean basins[9].

Previous estimates suggest the Weddell Sea provides ~60% of the total 8.1 Sv (1 Sv = 10^6 m^3 s^{-1}) of Antarctic Bottom Water (AABW) formed in the Southern Ocean[1], with most of the remainder formed in the Ross Sea and off Adélie Land[1,10]. The abyssal chlorofluorocarbon (CFC) distribution shows that AABW is exported to lower latitudes by two DWBCs[1]. The first transports Weddell Sea AABW along the Antarctic Peninsula and South Sandwich Island arc to ventilate the deep waters of the Atlantic and western Indian Ocean[11]. The second transports Ross Sea and Adélie Land AABW equatorward east of the Kerguelen Plateau, before passing through fracture zones in the mid-ocean ridge systems to supply the abyssal layers of the eastern Indian and Pacific Oceans[1,5,12] (Fig. 1a). The Kerguelen DWBC also returns the poleward flow

carried by a deep cyclonic gyre in the interior of the Australian Antarctic Basin (AAB). The high concentration of CFCs near the sea floor[1,13] in the AAB indicates it is the best-ventilated deep basin around Antarctica.

Current-meter moorings have confirmed the presence of a DWBC carrying dense water equatorward in the northwest Weddell Sea[11,14] and north of the Falkland Islands[8] (Supplementary Table 1). Ship-based synoptic "snapshots" have confirmed the presence of a DWBC east of the Kerguelen Plateau[2-7], but no time-series measurements have been made to allow estimates of its mean flow and variability. To estimate this flow, we deployed an array of eight closely-spaced current-meter moorings on the eastern flank of the plateau from February 2003 to January 2005 (Figs. 1b, 2). The horizontal coherence and duration of the array allowed accurate estimates of the transport and structure of the Kerguelen DWBC.

The DWBC forms a narrow (~50 km wide), intense, bottom-intensified flow to the northwest over the lower flank of the plateau, with a flow to the southeast further offshore (Fig. 2). The currents are remarkably strong for these depths: maximum two-year mean speed exceeds 20 cm s^{-1} at ~3500 m depth at M6 (the largest DWBC speeds yet observed at similar depths; Supplementary Table 1), much stronger than measured in the DWBC exporting AABW from the Weddell Sea[8,11,14]. The mean distribution of potential temperature (θ) shows that AABW (defined as $\theta < 0$°C following ref. 15) exists below 2500 m, forming a layer 1500 m thick off the continental rise (Fig. 2). Mean near-bottom potential temperatures at M3-5 are ~ –0.35°C. The isotherms slope up to the west with the coldest and thickest AABW layer over the lower flank of the plateau.

Three snapshots of the potential temperature and velocity field obtained from conductivity-temperature-depth (CTD) profiler and lowered acoustic Doppler current profiler (ADCP) sections during the experiment show a similar structure to the mean field derived from the mooring data, confirming the barotropic nature of the DWBC, with northwestward flow extending throughout the water column (an example in ref. 6). The similarity between the moored results and the synoptic snapshots indicates that the limited vertical resolution of the moored instruments is sufficient to capture the DWBC structure.

The daily velocity and potential temperature data are used to calculate the

AABW transport per unit width (Fig. 3a). The northwestward transport of AABW is concentrated between M4 and M6, with the largest value observed at M5 where the velocities are large and the AABW layer is thick (Fig. 2). Northwestward transport is commonly observed to extend offshore as far as M3 (~38 km from M5) and occasionally as far as M2 (~77 km from M5). A spectral analysis indicates that the DWBC transport is modulated by fluctuations with a period of ~20-40 days, likely reflecting the presence of topographic waves (e.g., ref. 16); the magnitude of the fluctuations is largest in the core of the DWBC near the base of the sloping topography and declines offshore. Overall, however, the core of the DWBC is relatively steady in both location and magnitude. The sense of the flow is reversed further offshore, reflecting the presence of the deep expression of branches of the Southern Antarctic Circumpolar Current Front (SACCF) and Polar Front (Fig. 1b), which cross the array from northwest to southeast at the eastern end of the array, the cyclonic gyre in the AAB[5] and possibly a local recirculation[6].

The total northwestward AABW transport, integrated from the inshore edge of the array (M8) to the zero-crossing point from northwestward to southeastward flow (see Methods), varies from 0.1 to 30.3 Sv (light blue curve, Fig. 3b) around an overall mean value of 12.3 Sv (dark green line), with a standard deviation of 5.6 Sv. The zero-crossing point is generally located just to the south of the northern branch of the SACCF and fluctuations in its position correspond with shifts in the front (green curve, Fig. 3a). Variability with time scales of ~20-40 days is clearly dominant, but lower frequency variability is also observed and largely reflects the influence of eddies and fronts of the ACC (as seen in satellite altimeter data, not shown). For example, the northwestward transport of AABW is briefly reduced to values less than 2 Sv on four occasions, each of which coincides with onshore translations of the ACC fronts or eddies (Fig. 3). Maxima in transport are observed when the presence of a cyclonic eddy over the eastern side of the array reinforces the northwestward flow. There is little evidence of seasonal variability. Despite the energetic variability, the mean flow is well-defined and the 95% confidence intervals (with the de-correlation time of 8.5 days) are narrow (±1.2 Sv). The cumulative average of the transport estimates (green curve) is within the 95% confidence intervals of the mean after 9 months, indicating that the records are of sufficient length to establish a stable mean. The overall impression is of a narrow, intense and relatively steady deep boundary current, modulated by topographic waves and the episodic influence of fronts and meanders of the ACC. This DWBC is associated with a mean temperature transport of -2.52±0.26 Sv °C

northwestward.

Snapshot estimates based on CTD/ADCP measurements are in agreement with the observations from the moored array, with the exception of the deployment cruise (Fig. 3b, Supplementary Table 2). However, these estimates sampled periods of larger than average transport (Fig. 3b) and hence give a larger and misleading impression of the strength of the mean flow. Long time-series are essential to determine robust mean values of variable ocean currents like the Kerguelen DWBC.

The southeastward flow across the eastern end of the array returns some AABW to the south. Integrating northeastwards from M8 and including the southeastward transport, the mean net northwestward transport of AABW reaches a maximum of 10.3 Sv (with a standard deviation of 4.7 Sv) at M3 and is 6.8 Sv across the entire array (standard deviation 7.9 Sv) (Fig. 3c). The southeastward flow reflects deep flow associated with the ACC and local[6] or basin-scale[5] recirculations; a portion of this flow may turn back to the north, east of the array[5,6]. Recirculation gyres offshore of DWBCs are predicted by theory[9] and frequently observed[17-20], and make it difficult to estimate the net throughflow of the deep OC[17]. Property distributions show that recently-ventilated AABW carried north in the DWBC exits the basin through fracture zones in the ridge to supply the deep southeast Indian Ocean, the Tasman Sea and the Pacific Ocean[5]. However, there are no quantitative estimates of the mean export of AABW through the fracture zones.

Several factors make it difficult to assess the relative contribution of the Kerguelen DWBC to the Southern Ocean overturning. These include the presence of recirculation gyres, interaction between the DWBC and other circulation regimes (e.g., the ACC and subpolar gyres)[8], the fact that mixing and entrainment change the volume and properties of AABW along the export pathway[13], and the lack of coherent long-term observations in other DWBCs. The only previous coherent current meter measurements of AABW export by a DWBC south of 45°S were obtained north of the Falkland Plateau, where a net transport of 1.9 Sv of Weddell Sea Deep Water ($\theta < 0.2$°C) was found to enter the Argentine Basin (the difference between 8.2 Sv westward and 6.3 Sv recirculating to the east)[8]. In comparison, the net transport of water with $\theta < 0.2$°C by the Kerguelen DWBC is 8.0 Sv (16.4 Sv to the northwest and an 8.4 Sv recirculation to the southeast). Incoherent multi-year moored measurements in the northwest Weddell Sea reveal relatively weak currents (deep mean flows < 7 cm s^{-1})[11]. Combining these

current-meter data with CTD sections gives a net export of 3.8 Sv of AABW ($\theta < 0°C$) from the Weddell Sea[14]; based on an inverse model, an additional 4.7 Sv may leave the Weddell Sea across the Scotia Ridge[21]. Estimates of AABW ($\theta < 0°C$) export from the Weddell Sea derived from alternative approaches (e.g., mass and tracer budgets or inverse models) vary by a factor of 3 (from 3.3 to 10.0 Sv)[21]. While the lack of long-term, coherent velocity measurements spanning the boundary current and offshore recirculations makes it difficult to be definitive about the relative size of the Atlantic and Kerguelen DWBCs, we can conclude that the two are at least comparable in magnitude.

Recognition of the importance of the OC in the climate system and its potential vulnerability has driven enhanced efforts to obtain long-term measurements of the DWBC system in the North Atlantic (e.g., the RAPID/MOCHA program[22-24]). The Southern Ocean limb of the overturning ventilates the deep ocean at about the same rate as the North Atlantic[13], is dynamically coupled to the Atlantic overturning[25], and is also potentially sensitive to future climate change[26,27]. Understanding of the global OC and its response to changes in forcing therefore requires an observing system that provides sustained measurements of the main pathways of the OC in both hemispheres. Our results show that the Kerguelen DWBC is one of these major pathways. The demonstration that robust transport estimates can be made with simple, coherent arrays of current-meter moorings provides a guide to the type of sustained measurements needed at this and other locations in the Southern Ocean.

METHODS

Eight moorings containing 31 current meters (Aanderaa RCM-5 and 8), 2 ADCPs (RD Instruments WH-Sentinel 300 kHz), 33 conductivity-temperature (CT) recorders (SeaBird SBE 37), and 2 thermistors (SeaBird SBE 39) were deployed and recovered by RSV Aurora Australis in February 2003 and January 2005 (Fig. 2). Valid data were obtained by most of the instruments; instruments with gaps are indicated in Fig. 2. Top-to-bottom temperature and salinity profiles were taken by a CTD profiler (SeaBird SBE 911plus) during the deployment and recovery cruises and the BEAGLE2003 cruise by R/V Mirai in February 2004. Near-surface and full-depth velocity data taken by shipboard (RDI broadband 75 kHz) and lowered (RD Instruments WH-Sentinel 300 kHz) ADCPs during the BEAGLE2003 cruise are used. Near-surface and full-depth velocity data taken by shipboard (RDI narrowband 150 kHz) and lowered ADCPs (SonTek ADP 250 kHz) during the deployment and recovery cruises are also used.

Instrument depths are estimated using pressure values measured by the current meters (mostly second instrument from the top) and assuming that moorings remained straight though with tilt. (Nominal instrument depths are used during the entire mooring period at M8 due to the failed pressure sensor.) For the water column above the uppermost CT recorder at each mooring, temperature data from current meters and thermistors are used. These temperature data are converted to potential temperature (the temperature of the water parcel if it was raised adiabatically to the surface) using the average salinity at the same pressure among the three CTD observations in February 2003 and 2004, and January 2005. For the water column below the uppermost CT recorder, potential temperature values derived at CT recorders are only used. Note that the assumption of nominal instrument depths at M8 and the use of potential temperature data converted with the average CTD data have minimal effects on the resulting AABW volume transport estimate because AABW mostly exists below 2500 m and away from M8 (Fig. 2). 2-hourly data of velocity perpendicular to the mooring array and potential temperature were calculated in 10-m vertical bins between depths of 900 m and the bottom, mostly by interpolation and slightly by extrapolation above (below) the uppermost (lowermost) valid data.

Using these vertically-binned data at each mooring and cross-sectional areas between adjacent moorings, daily AABW volume transports ($\theta < 0$ °C) are calculated by integrating from M8 over the slope to the zero-crossing point from the northwestward to southeastward transport (Fig. 3). Estimation of the net AABW transport is

complicated by several factors, including the presence of recirculation gyres, upper ocean currents (e.g., fronts of the ACC) opposing or enhancing the deep flow and synoptic variability such as eddies and frontal meanders. Integrating to the zero-crossing point, as done here, is a commonly used approach (e.g., ref. 17) that permits comparison to other studies, but remains somewhat arbitrary. The coincidence of the zero-crossing point with the location of the northern branch of the SACCF, which carries AABW to the southeast, provides further oceanographic support for choosing the zero-crossing point as the offshore edge of the DWBC. We explored several alternative methods of integrating the AABW transport. The time-mean of the sum of all northwestward flow of AABW across the array gives 12.9 Sv (compared to 12.3 Sv inshore of the zero-crossing point). The difference in the mean between this northwestward flow and the sum of all the southeastward flow (6.0 Sv) is the net northwestward flow (6.8 Sv) across the array. Using the mean velocity and potential temperature sections, and integrating northwestward flows to the zero-crossing point, gives 10.4 Sv. (The difference between estimates using the mean fields and the full time series reflects the fact that both the area and velocity of the AABW layer differ in the two cases, in part because the mean field includes periods of southeastward flow.) The AABW transports from ref. 6 shown in Fig. 3b and Supplementary Table 2 were re-calculated using a potential temperature of 0°C to define AABW.

The location of the ACC fronts (Figs. 1b, 3a) are identified as specific values of the absolute sea surface height (SSH) field (e.g., ref. 28). The SSH field is derived from the combination of CLS/AVISO "Mean Sea Level Anomaly" maps, which are produced by mapping data from the TOPEX/POSEIDON, ERS-1 and ERS-2 satellite altimeters[29], and the mean dynamic height data from the climatology of ref. 30.

Additional information

The authors declare no competing financial interests. Correspondence and requests for materials should be addressed to Y. F..

Acknowledgements

We are deeply indebted to Danny McLaughlan and Kevin Miller for their mooring works. Thanks are extended to the officers, crew and scientists on board RSV Aurora Australis for their help with field observations. Discussions with Genta Mizuta and Yuji Kashino were helpful. Figure 1a was drawn by Louise Bell and Kyoko Kitagawa. Other figures were produced by the PSPLOT library written by Kevin E. Kohler. In Japan support was provided by Grants-in-Aid 14403006, 17340138, 20244075, 20540419, and 21310002 for Scientific Research from Ministry of Education, Science, Sports and Culture. In Australia support was provided by the Cooperative Research Centre program of the Australian government and by the Australian National Antarctic Research Expeditions; this work is a contribution to the Australian Climate Change Science Program, funded jointly by the Department of Climate Change, the Bureau of Meteorology and CSIRO.

Author contributions

J.A.C., M.W., S.R.R. and Y.F. planned the experiment; M.R., Y.F., S.R.R., J.A.C., S.A. and S.S. carried out the observations; Y.F., M.R., S.S. and S.A. carried out data processing; Y.F., S.R.R., J.A.C., S.S. and M.W. wrote the manuscript, with other authors commenting.

References

1. Orsi, A. H., Johnson, G. C. & Bullister, J. L. Circulation, mixing, and production of Antarctic Bottom Water. *Prog. Oceanogr.* **43,** 55-109 (1999).

2. Speer, K. G. & Forbes, A. A deep western boundary current in the South Indian Basin. *Deep-Sea Res. I* **41,** 1289-1303 (1994).

3. Donohue, K., Hufford, G. E. & McCartney, M. S. Sources and transport of the deep western boundary current east of the Kerguelen Plateau. *Geophys. Res. Lett.* **26,** 851-854 (1999).

4. Narumi, Y., Kawamura, Y., Kusaka, T., Kitade, Y. & Nagashima, H. The Deep Western Boundary Current along the eastern slope of the Kerguelen Plateau in the Southern Ocean: observed by the Lowered Acoustic Doppler Profiler (LADCP). *La Mer* **43,** 49-59 (2005).

5. McCartney, M.S. & Donohue, K. A. A deep cyclonic gyre in the Australian-Antarctic Basin. *Prog. Oceanogr.* **75,** 675-750 (2007).

6. Aoki, S. et al. Deep western boundary current and southern frontal systems of the Antarctic Circumpolar Current southeast of the Kerguelen Plateau. *J. Geophys. Res.* **113,** doi:10.1029/2007JC004627 (2008).

7. Park, Y.-H., Vivier, F., Roquet, F. & Kestenare, E. Direct observations of the ACC transport across the Kerguelen Plateau. *Geophys. Res. Lett.* **36,** L18603, doi:10.1029/2009GL039617 (2009).

8. Whitworth III, T., Nowlin, W. D., Pillsbury, R. D., Moore, M. I. & Weiss, R. F. Observations of the Antarctic Circumpolar Current and deep boundary current in the Southwest Atlantic. *J. Geophys. Res.* **96,** 15105-15118 (1991).

9. Stommel, H. & Arons, A. B. On the abyssal circulation of the World Ocean - I. Stationary planetary flow patterns on a sphere. *Deep-Sea Res.* **6,** 140-154 (1960).

10. Rintoul, S. R. On the origin and influence of Adélie Land Bottom Water in *Ocean, Ice, and Atmosphere: Interactions at the Antarctic Continental Margin.* (eds Jacobs,

S. S. & Weiss, R. R.) 151-171 (*Antarct. Res. Ser.* **75,** American Geophysical Union, Washington, DC, 1998).

11. Fahrbach, E., Harms, S. Rohardt, G., Schröder, M. & Woodgate, R. A. Flow of bottom water in the northwestern Weddell Sea. *J. Geophys. Res.* **106,** 2761-2778 (2001).

12. Nakano, H. & Suginohara, N. Importance of the eastern Indian Ocean for the abyssal Pacific. *J. Geophys. Res.* **107,** 3219, doi:10.1029/2001JC001065 (2002).

13. Orsi, A. J., Smethie Jr., W. M. & Bullister, J. L. On the total input of Antarctic waters to the deep ocean: A preliminary estimate from chlorofluorocarbon measurements. *J. Geophys. Res.* **107,** doi:10.1029/2001JC000976 (2002).

14. Fahrbach, E., Rohardt, G., Schröder, M. & Strass, V. Transport and structure of the Weddell Gyre. *Ann. Geophysicae* **12,** 840-855 (1994).

15. Carmack, E. C. Water characteristics of the Southern Ocean south of the Polar Front, in Voyage of Discovery, edited by M. Angel. *Deep-Sea Res.* **24,** suppl., 15-37 (1977).

16. Moore, M. I. & Wilkin, J. L. Variability in the South Pacific Deep Current from current meter observations and a high-resolution global model. *J. Geophys. Res.* **103,** 5439-5457 (1998).

17. Schott, F. A. et al. Circulation and deep-water export at the western exit of the subpolar north Atlantic. *J. Phys. Oceanogr.* **34,** 817-842 (2004).

18. Bryden, H. L., Johns, W. E. & Saunders, P. M. Deep western boundary current east of Abaco: Mean structure and transport. *J. Mar. Res.* **63,** 35-57 (2005).

19. Schott, F. A., Fisher, J., Dengler, M. & Zantopp, R. Variability of the Deep Western Boundary Current east of the Grand Banks. *Geophys. Res. Lett.* **33,** L21S07, doi:10.1029/2006GL026563 (2006).

20. McCartney, M. S. Recirculating components of the deep boundary current of the

northern North Atlantic. *Prog. Oceanogr.* **29,** 283-383 (1992).

21. Naveira Garabato, A. C., McDonagh, E. L., Stevens, D. P., Heywood, K. J. & Sanders, R. J. On the export of Antarctic Bottom Water from the Weddell Sea. *Deep-Sea Res. II* **49,** 4715-4742 (2002).

22. Cunningham, S. A. et al. Temporal variability of the Atlantic meridional overturning circulation at 26.5°N. *Science* **317,** 935-938 (2007).

23. Kanzow, T. et al. Observed flow compensation associated with the MOC at 26.5°N in the Atlantic. *Science* **317,** 938-941 (2007).

24. Johns, W. E. et al. Variability of shallow and deep western boundary currents off the Bahamas during 2004-05: Results from 26°N RAPID-MOC array. *J. Phys. Oceanogr.* **38,** 605-623 (2008).

25. Weaver, A. J., Saenko, O. A., Clark, P. U. & Mitrovica, J. X. Meltwater pulse 1A from Antarctica as a trigger of the Bølling-Allerød warm interval. *Science* **299**, 1709–1713 (2003).

26. Meehl, G. A. et al. Global Climate Projections. In: *Climate Change 2007: The Physical Science Basis. Contribution of Working Group I to the Fourth Assessment Report of the Intergovernmental Panel on Climate Change* (eds Solomon, S. et al.) (Cambridge Univ. Press, Cambridge and New York, 2007).

27. Sen Gupta, A. et al. Projected changes to the Southern Hemisphere ocean and sea ice in the IPCC AR4 climate models. *J. Clim.* **22,** 3047-3078 (2009).

28. Sokolov, S. & Rintoul, S. R. The circumpolar structure and distribution of the Antarctic Circumpolar Current fronts. Part 1: Mean circumpolar paths. *J. Geophys. Res.* **114,** C11, doi:10.1029/2008JC005248 (2009).

29. Le Traon, P., Nadal, F. & Ducet, N. An improved mapping method of multisatellite altimeter data. *J. Atmos. Ocean. Technol.* **15,** 522-534 (1998).

30. Gouretski, V. V. & Koltermann, K. P. WOCE Global Hydrographic Climatology. *A*

Technical Report **35,** Berichte des BSH (2004).

Figure Legends

Figure 1 | Maps of the Indian and Pacific sectors of the Southern Ocean and the region around the Kerguelen Plateau. **a,** A schematic view of AABW sources and boundary currents carrying AABW. The region in Fig. 1b is indicated by the red box. **b,** Mooring locations (red) and CTD stations used to estimate transport during the WOCE I8S (green, ref. 3) and BEAGLE2003 (blue, ref. 6) cruises. Locations of branches of the Polar Front and the Southern ACC Front are drawn after ref. 28.

Figure 2 | Mean sections of velocity and potential temperature. The mean sections of the velocity perpendicular to the mooring array (shading; positive northwestward) and potential temperature (contours) over the entire duration. Also shown is a schematic diagram of moorings. CM, CT and TM denote current meter, conductivity-temperature recorder and thermistor. Ratios of valid velocity data are indicated by three symbols.

Figure 3 | Antarctic Bottom Water (AABW) transport. **a,** Daily transport per unit width (Sv km^{-1}); positive northwestward (blue). ACC fronts are shown in the same colors as in Fig. 1b. **b,** Daily (light blue) and low-passed volume transport (dark blue, 40-day Butterworth filter). Cumulative mean (green) and overall mean (dark green) with 95% confidence limit (dark green dashed). Dots are snapshot estimates from hydrographic sections referenced to shipboard (orange) and lowered (red) ADCP data. Estimates from WOCE in 1994-95[3] are shown on left axis. **c,** Cumulative net AABW volume transport from M8 (curve) and standard deviation (bars).

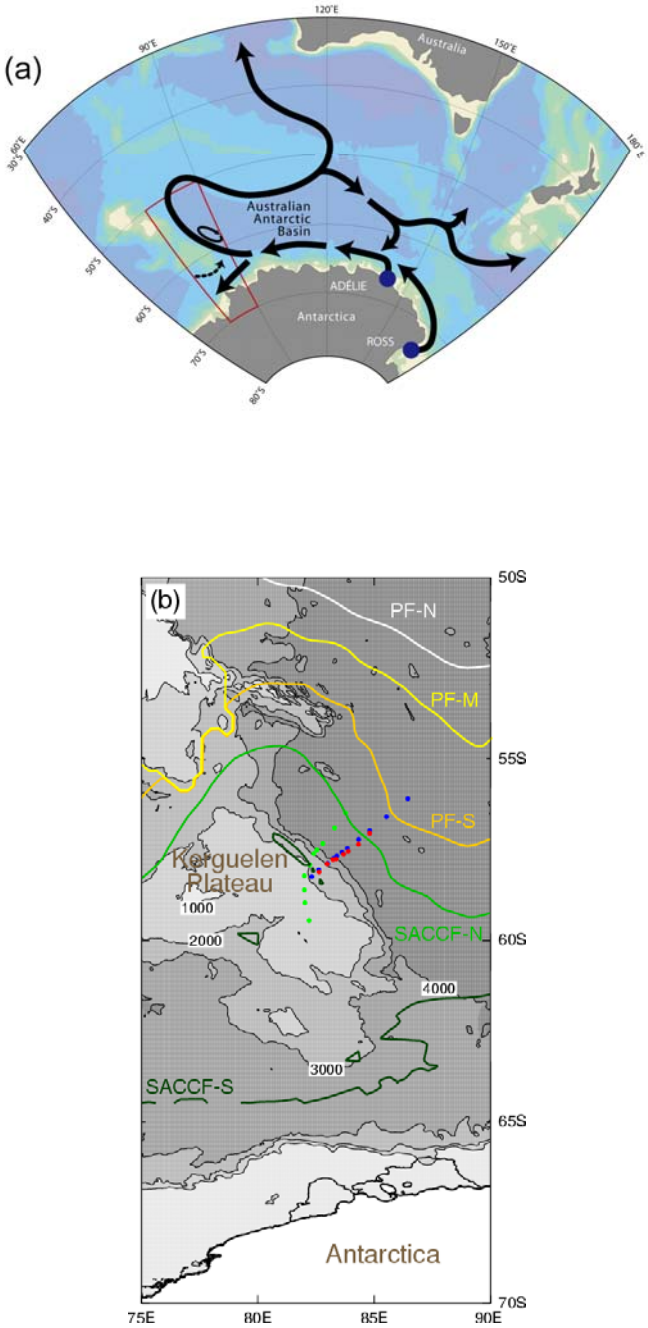

Figure 1 | Maps of the Indian and Pacific sectors of the Southern Ocean and the region around Kerguelen Plateau.

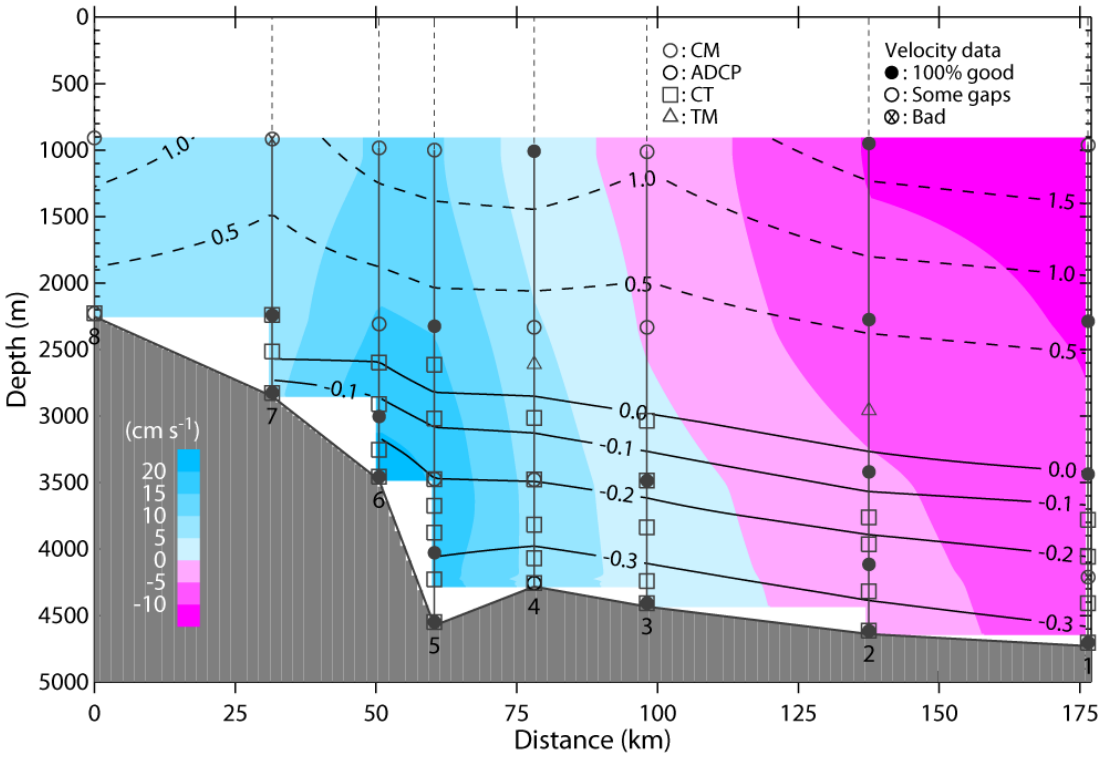

Figure 2 | Mean sections of velocity and potential temperature.

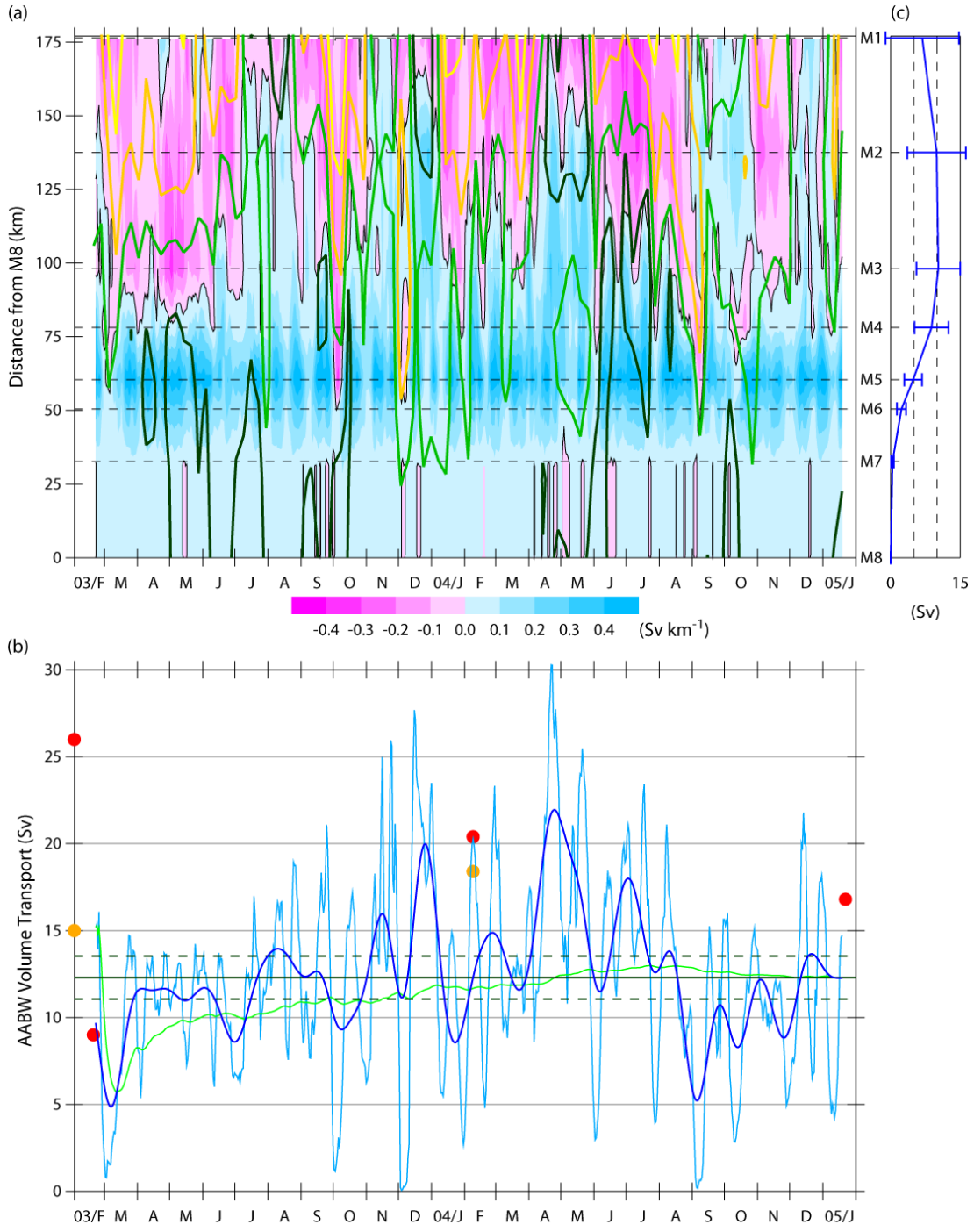

Figure 3 | Antarctic Bottom Water (AABW) transport.

Supplementary Table 1: Maximum observed mean speeds in deep western boundary currents at depths greater than 3000 m, for which time-series measurements of at least one year in length exist. Also shown are those of deep channel flows (indicated by asterisk) for comparison. Water mass abbreviations: Antarctic Bottom Water (AABW), Weddell Sea Bottom Water (WSBW), Circumpolar Deep Water (CDW), North Atlantic Deep Water (NADW).

Location	**Water mass**	**Max. mean speed (cm s^{-1})**	**Depth (m)**	**Duration (days)**	**Reference**
Kerguelen DWBC	AABW	23.6	3461	699	This paper
North of Falklands	AABW	10-15	~5500	409	Ref. 8: Whitworth et al. (1991)
Northwest Weddell Sea	WSBW	6.3	3474	688	Ref. 11: Fahrbach et al. (2001)
South Pacific DWBC	CDW	9.6	5134	663	Ref. 31: Whitworth et al. (1999)
Hunter Channel (South Atlantic 34°S)*	AABW	7.1	4175	518	Ref. 32: Zenk et al. (1999)
Vema Channel (South Atlantic 31.1°S)*	AABW	33.7	4425	692	Ref. 33: Hogg et al. (1999)
North Atlantic (42°N)	NADW	9.3	4200	2 yrs	Ref. 19: Schott et al. (2006)
North Atlantic (26.5°N)	NADW	13.9	3080	1552	Ref. 18: Bryden et al. (2005)
North Atlantic (26.5°N)	NADW	~ 14	4000	~385	Ref. 24 Johns et al. (2008)

Supplementary Table 2: Northwestward transport of AABW ($\theta < 0$°C; in Sv) in the Kerguelen DWBC. The WOCE I8S section (green dots, Fig. 1b) crossed the DWBC downstream of the moored array. The other sections were aligned with the moored array. For the WOCE I8S section, shipboard ADCP (SADCP) and lowered ADCP (LADCP) estimates were obtained by referencing geostrophic calculations to SADCP and LADCP measurements, respectively. Other LADCP estimates are obtained without geostrophic calculations. Mooring estimates during the concurrent cruises are based on the data around the CTD/LADCP measurements except that most of the CTD/LADCP observations on the deployment cruise were completed several days prior to the mooring deployment.

Voyage	**Date**	**SADCP**	**LADCP**	**Moorings**
WOCE I8S[3]	Dec 1994 − Jan 1995	15.0±3.2	26.0±4.4	
Mooring deployment	Feb 2003		9.0	15.2
BEAGLE2003[6]	Feb 2004	18.5	20.4	20.5
Mooring recovery	Jan 2005		17.4	16.8
Two-year mean	Feb 2003 – Jan 2005			12.3±1.2 (std. dev.: 5.6)

Supplementary Information References

31. Whitworth III, T. et al. On the deep western-boundary current in the Southwest Pacific Basin. *Prog. Oceanogr.* **43,** 1-54 (1999).

32. Zenk, W., Siedler, G. & Lenz, B. Antarctic Bottom Water flow through the Hunter Channel. *J. Phys. Oceanogr.* **29,** 2785-2801 (1999).

33. Hogg, N., Siedler, G. & Zenk, W. Circulation and variability at the southern boundary of the Brazil Basin. *J. Phys. Oceanogr.* **29,** 145-157 (1999).